NANO LETTERS

2004
Vol. 4, No. 4
753−756

Carbon Nanotube Transistor Operation at 2.6 GHz

Shengdong Li,[†] Zhen Yu,[†] Sheng-Feng Yen,[†] W. C. Tang,[†,‡] and Peter J. Burke*[,†,‡]

Integrated Nanosystems Research Facility, Electrical Engineering and Computer Science, and Biomedical Engineering, University of California, Irvine, California 92697

Received January 20, 2004; Revised Manuscript Received February 18, 2004

ABSTRACT

We present the first demonstration of single-walled carbon nanotube transistor operation at microwave frequencies. To measure the source-drain ac current and voltage at microwave frequencies, we construct a resonant LC impedance-matching circuit at 2.6 GHz. Both semiconducting and metallic nanotubes are measured. Varying the back-gate voltage for a semiconducting nanotube at dc varies the 2.6-GHz source-drain impedance. In contrast, varying the back-gate voltage on a metallic nanotube at dc has no effect on the microwave source-drain impedance. We find the ac source-drain impedance to be different than the dc source-drain resistance, which may be due to the distributed nature of the capacitive and inductive impedance of the contacts to the nanotube.

The dynamical (ac) electrical properties of carbon nanotubes are technologically relevant for both active and passive devices made from carbon nanotubes. At dc, it is known that electrons can move without scattering over many micrometers inside a carbon nanotube.[1] We recently analyzed, from a theoretical point of view, the microwave passive[2,3] and active[4,5] electrical properties of nanotubes in some detail. The successful operation of a multiwalled carbon nanotube rf single-electron transistor was recently reported.[6] In this paper, we present the first measurements of the electrical properties of single-walled nanotubes at gigahertz frequencies.[7] In so doing, we demonstrate, for the first time, the operation of single-walled nanotube transistors at microwave frequencies.

Our nanotubes were grown from lithographically patterned nanoparticle catalyst sites using CVD.[8] The nanotube growth procedure and recipes are described in detail in ref 9. Electrical contact was achieved with evaporated Ti/Au electrodes using optical lithography. An SEM was used to locate the nanotubes before the electrical contact, and the catalyst pattern was used to align the contacts to the nanotubes. The metallic nanotube was annealed at 600 °C in Ar for 5 min; the semiconducting nanotube was not annealed. The electrode pattern consisted of an ∼1 mm × ∼1 mm contact pad.

SEM images of two nanotube devices grown are shown in Figures 1 and 2. Both devices were fabricated simultaneously on the same wafer and were separated by cleaving after the fabrication process. This means that they were both grown in the same growth run and that the metal was evaporated onto both samples in the same metallization procedure. The diameter of nanotubes grown under similar conditions in our lab was less than 1.5 nm as measured with an AFM, which leads us to conclude that the nanotubes shown are single-walled nanotubes.

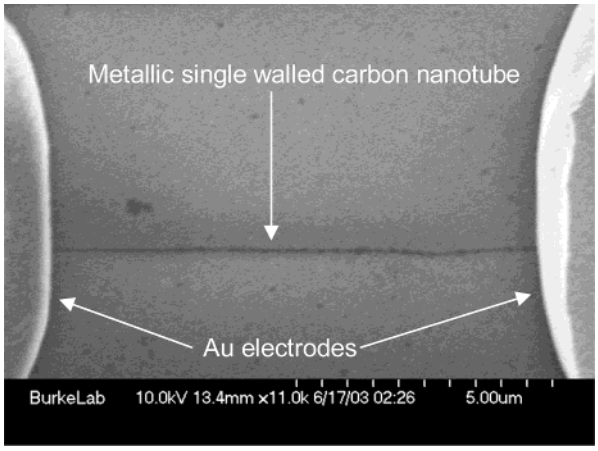

Figure 1. SEM image of the metallic single-walled carbon nanotube used in these studies.

We measure the microwave reflection coefficient defined as $S_{11} = (Z_L - 50\ \Omega)/(Z_L + 50\ \Omega)$ off of the nanotube and matching circuit, as in ref 10. Here, Z_L is the impedance of the load attached to the end of a coaxial cable. The load consists of the nanotube and an LC impedance-matching circuit. The wire bonds used to connect the device served as the inductor, and the on-chip capacitance to ground served

* Corresponding author. E-mail: pburke@uci.edu. Phone: 949-824-9326. Fax: 949-824-3732.
[†] Electrical Engineering and Computer Science.
[‡] Biomedical Engineering.

10.1021/nl0498740 CCC: $27.50
Published on Web 03/23/2004

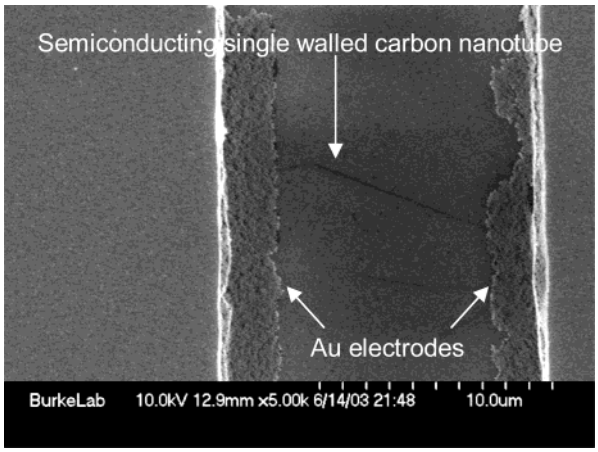

Figure 2. SEM image of the semiconducting single-walled carbon nanotube used in these studies.

as the capacitor. On resonance, the impedance-matching circuit transforms the nanotube dynamical impedance down from a high value to close to 50 Ω. We performed our measurements at both room temperature and 4 K. At room temperature, the substrate losses dominated the microwave properties. In this paper, we focus on the performance at 4 K.

The details of the test fixture and matching circuit are as follows: A microstrip launcher was used to connect a 1-m-long semirigid coaxial cable (UT-141, Microcoax) to a 1-cm length of a Cu microstrip on a 0.5-mm-thick Duroid substrate. The test fixture used was characterized extensively in ref 11. There, it was shown to provide well-controlled microwave coupling up to 40 GHz. For measurements at 4 K, the cable was used to insert the test fixture directly into a liquid-He storage dewar.

The Si wafer with the nanotube devices was cleaved into 2×2 mm^2 pieces and abutted to the end of the microstrip. The plane of the microstrip and the surface of the Si wafer were at the same height above the brass test fixture. Because the substrate was used as a gate and the test fixture was grounded, we used a thin piece of Cu tape on the back side of the substrate to provide electrical contact to the substrate and to insulate the substrate from ground.

To contact the sample electrically, 25-μm-diameter gold wires of ~2-cm length were soldered from the end of the microstrip to one of the electrical contact pads and from the other electrical contact pad to the ground plane. These provided the inductors that formed approximately 10 nH of inductance in series with the nanotube. When we measured the same sample mounted with In solder (which has very little inductance) instead of wire bonds, the resonance dip in S_{11} (see below) disappeared, thus verifying that the Au wires served as inductors. The excess capacitance to ground from the electrical contact pads is estimated to be ~0.1 pF from the geometry.

The impedance-matching equivalent circuit is shown in Figure 3. We measured the S_{11} off of this circuit using a control sample with the same electrode pattern as that of the nanotube device (but no nanotube) and found that there is still dissipation in the resonator (i.e., a finite Q). We

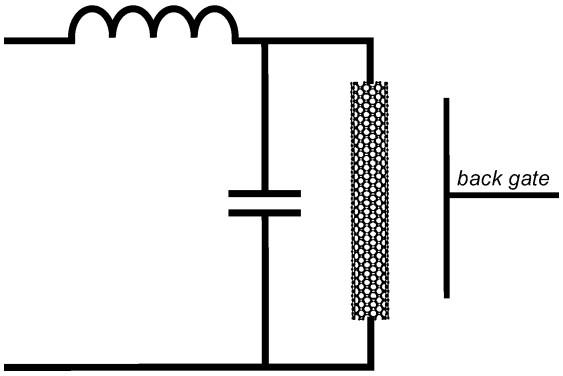

Figure 3. Equivalent circuit for the resonator.

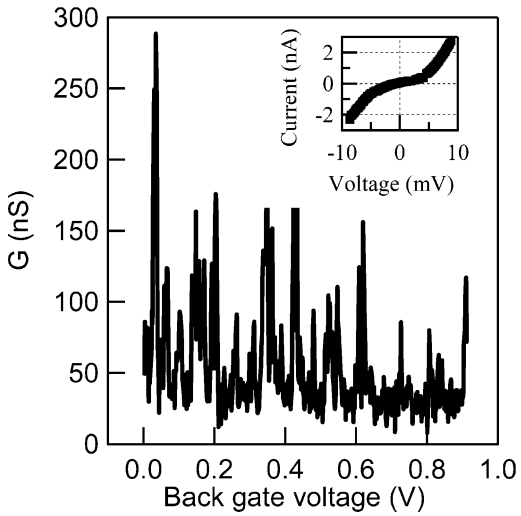

Figure 4. dc electrical properties of the semiconducting nanotube.

attribute this to radiation losses into free space (radiation resistance) from the wires. Numerically, this radiation resistance is ~10 kΩ and varies with the length of wire used.

We turn our attention now to the semiconducting nanotube. The semiconducting nanotube had a room-temperature resistance of 300 kΩ and behaved as a p-type device when using the substrate as a back-gate, consistent with previously measured results.[1] Because the nanotube could be gated at room temperature, we have characterized it as a semiconducting nanotube.

We plot in Figure 4 the 4 K conductance versus back-gate voltage. The inset shows the nanotube $I-V$ curve. The structure is due to a combination of Coulomb-blockade[12] (single-electron transistor) effects, quantum interference of the electron wave functions,[13] and depletion of the charge carriers[14] in the nanotube. At room temperature, the depletion curve was smooth, with no fine structure.

A critical issue is how the nanotube contacts the Au electrically. At dc, the theoretical lower limit for the nanotube resistance is $h/4e^2 = 6.2$ kΩ. At ac, the theory is much more complicated.[3] For the nanotubes we present in this work, the nanotube extended under the Au contact pads by at least 5 μm. Thus, even though the dc resistance is high (~1 MΩ, see below), most likely dominated by contact resistance, there may be an additional capacitive electrical contact to the nanotube if the evaporated Au does not destroy the nanotube.

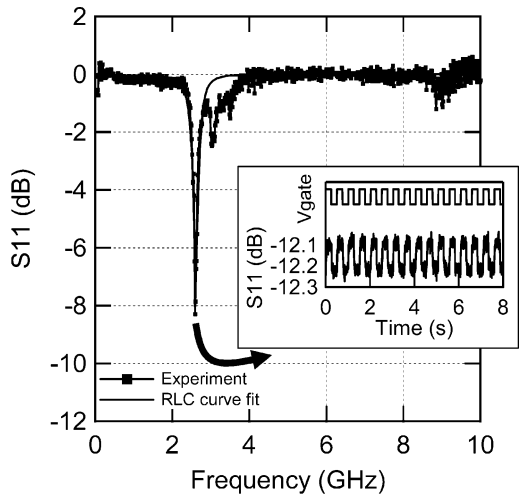

Figure 5. Measured S_{11} for the semiconducting nanotube resonator. The time domain measurement is exactly on resonance, whereas the frequency domain measurement missed the resonance frequency because of the finite point density.

Indeed, other SEM and AFM images (not shown) indicate that the nanotube is still intact under the Au electrodes.

In Figure 5, we plot the measured S_{11} versus frequency for the semiconducting nanotube. A clear resonance is visible at 2.6 GHz, where the impedance-matching circuit transforms the nanotube impedance to ~50 Ω. By applying a voltage of 10 V_{pp} to the substrate, we are able to consistently change the measured value of S_{11} on resonance with high reproducibility, as shown in the inset. This clearly demonstrates that varying the gate voltage at dc varies the 2.6-GHz source-drain impedance, thus verifying the microwave-frequency operation of a carbon nanotube transistor.

According to our calculations,[3,4] the ac impedance of a carbon nanotube should have significant real and imaginary components. In this work, the inductance in our matching circuit is set by the length of the wire bond, which is only approximately known. Thus, we cannot quantitatively determine which part of the inductance is due to the nanotube and which part is due to the wire bond. This issue will be addressed in future work with integrated, lithographically fabricated matching circuits. If we model the nanotube as shown in Figure 3 as a pure resistor and neglect the imaginary part, a three-parameter fit to the measured S_{11} data give values of $L = 40$ nH, $C = 0.1$ pF, and $R = 27$ kΩ. (The fitted curve is shown in Figure 5.) The fitted resistance is comparable to the radiation resistance for this circuit, indicating that the nanotube ac resistance is presumably much larger. This is consistent with the measured dc resistance of ~5 MΩ at 4 K.

We would like to correlate the nanotube ac performance with its dc electrical properties. If we assume that the dc resistance of the nanotube is the same as the ac resistance of the nanotube, then the effect of the gate voltage is to change the nanotube ac resistance from ~3 to >20 MΩ, as can be seen from Figure 4. For the microwave measurements, the radiation resistance (~27 kΩ for this circuit) is independent of the gate voltage. Because the radiation resistance is in parallel with the nanotube resistance, the effect of the

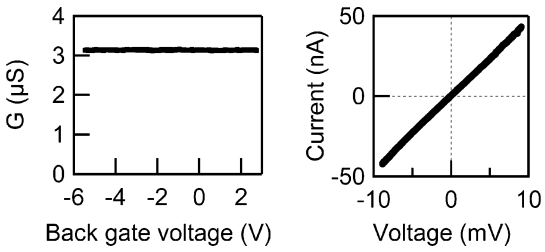

Figure 6. dc electrical properties of the metallic nanotube.

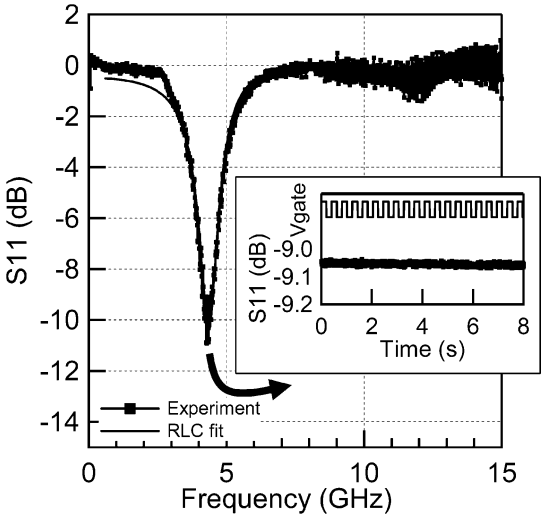

Figure 7. Measured S_{11} for the metallic nanotube resonator.

gate voltage is to modulate the net resistance by ~(27 kΩ||20 MΩ) − (27 kΩ||3 MΩ) ≈ 100 Ω. Numerically this would cause a change in S_{11} of ~0.01 dB. This is numerically about a factor of 10 smaller than the observed change in S_{11} of 0.1 dB. Thus, the nanotube ac electrical properties are different than the dc electrical properties. Possible reasons for this are discussed below.

We now turn our attention to the metallic nanotube. The metallic nanotube had a room-temperature resistance of 80 kΩ; this did not vary appreciably (less than 1%) with a back-gate voltage. Because the nanotube could not be gated at room temperature, we have characterized it as a metallic nanotube. We plot in Figure 6 the conductance versus gate voltage at 4 K, where it is seen that the nanotube conductance is independent of gate voltage. The $I-V$ curve (also shown in Figure 6) is linear.

In Figure 7, we plot the measured S_{11} versus frequency for the metallic nanotube. A clear resonance is visible at 4 GHz, where the impedance of the nanotube is transformed down to close to 50 Ω. The resonance frequency is slightly different because of the different length of wire used to mount this sample. In contrast to the semiconducting nanotube resonator, a voltage of 10 V_{pp} applied to the substrate does not change the measured value of S_{11} within the noise limits of 0.01 dB. If we model the nanotube as shown in Figure 3 as a pure resistor, then a three-parameter fit to the measured S_{11} data gives values of $L = 14$ nH, $C = 0.1$ pF, and $R = 1.7$ kΩ. The fitted curve is shown in Figure 7. The resistance is lower than the radiation resistance,

indicating that the nanotube ac resistance is indeed about 1.7 kΩ. This is significantly different from the nanotube dc resistance.

Thus, neither the dc nor ac electrical properties of the metallic nanotube depend on the back-gate voltage. In this sense, the dc and ac electrical properties are consistent. However, the absolute dc and ac electrical resistances are different.

We now discuss possible reasons for the difference between the measured dc and ac impedance. For the metallic nanotube in particular, the inferred resistance at ac is less than the theoretical Landauer−Buttiker formalism lower limit of $h/4e^2$. This is not an inconsistency with theory. Indeed, it is possible for a capacitively contacted nanotube (or any 1D conductor) with no scattering in the channel to have an ac impedance that is less than $h/4e^2$ because there is no contact resistance if the contact is only capacitive. From a theoretical point of view, if there is no scattering along the nanotube length and the nanotube is capacitively contacted, then at ac there should be no dissipation at all. Although we did not emphasize this point explicitly, we have previously provided extensive modeling of the effects of the distributed capacitive contacts on a nanotube.[2,3] In our nanotubes, there is clearly some dc contact resistance, but in addition, there may be significant capacitive coupling because the nanotube extends under the contacts by approximately 20 μm on each side. The metal was evaporated directly onto the nanotube, so the capacitive coupling should be strong.

Although we have clearly demonstrated the operation of a nanotube transistor at microwave frequencies, we have not fully characterized *all* of its ac properties. A full characterization would require measurements of the source-drain ac current, the source-drain ac voltage, the gate-source ac current, and the gate-source ac current and their relationship (a 2×2 matrix called the h matrix, or equivalently the impedance matrix, or equivalently the S matrix), all as functions of the dc gate bias, the dc drain bias, and frequency. What we have measured here is the ratio of the ac source-drain voltage to the ac source-drain current at 2.6 GHz, and we have shown that it depends on the dc gate voltage. These full characterization measurements, although challenging because of the high impedances involved, are clearly a topic for future research.

Acknowledgment. This work was supported by the Army Research Office (award DAAD19-02-1-0387), the Office of the Naval Research (award N00014-02-1-0456), and DARPA (award N66001-03-1-8914).

References

(1) McEuen, P. L.; Fuhrer, M.; Park, H. *IEEE Trans. Nano.* **2002**, *1*, 78−85.
(2) Burke, P. J. *IEEE Trans. Nano.* **2002**, *1*, 129−144.
(3) Burke, P. J. *IEEE Trans. Nano.* **2003**, *2*, 55−58.
(4) Burke, P. J. *Proc. − Int. Semicond. Device Res. Symp.* **2003**, 314−315 (invited).
(5) Burke, P. J. *Solid State Electron.*, in press, 2004.
(6) Roschier, L.; Hakonen, H.; Bladh, K.; Delsing, P.; Lehnert, K. W.; Spietz, L.; Schoelkopf, R. J. *J. Appl. Phys.* **2004**, *95*, 1274−1286.
(7) These measurements were also presented by one of us (Z.Y.) at the *3rd IEEE Conference on Nanotechnology*, San Francisco, CA, August 12−14, 2003.
(8) Kong, J.; Soh, H. T.; Cassell, A.; Quate, C. F.; Dai, H. *Nature* **1998**, *395*, 878.
(9) Li, S.; Yu, Z.; Gadde, G.; Burke, P. J.; Tang, W. C. *Proceedings of the 3rd IEEE Conference on Nanotechnology*, 2003.
(10) Burke, P. J.; Spielman, I. B.; Eisenstein, J. P.; Pfeiffer, L. N.; West, K. W. *Appl. Phys. Lett.* **2000**, *76*, 745−747.
(11) Burke, P. J. Ph.D. Thesis, Yale University, New Haven, CT, 1997 (unpublished).
(12) Park, J.; McEuen, P. L. *Appl. Phys. Lett.* **2001**, *79*, 1363−1365.
(13) Wenjie, L.; Bockrath, M.; Bozovic, D.; Hafner, J. H.; Tinkham, M.; Hongkun, P. *Nature* **2001**, *411*, 665−669.
(14) Durkop, T.; Getty, S. A.; Cobas, E.; Fuhrer, M. S. *Nano Lett.* **2003**, *4*, 35−39.

NL0498740